

Tensile Performance of Perforated IPE Connectors within Composite Beams

Rendimiento a la tracción de conectores IPE perforados en vigas compuestas

Boursas, F. ^{*1}; Boufarh, R. ^{*}; Maghaghi, B. ^{**}; Saidani, M. ^{***}

* Department of Civil Engineering, University of Larbi Tébessi Tébessa, Laboratoire de Génie Civil appliqué, Algeria.

** Civil Engineering Department, Ferhat Abbas-setif1 University, Setif 19000, Algeria.

*** School of Energy, Construction and Environment, Coventry University, Coventry, UK.

Fecha de Recepción: 08/03/2024

Fecha de Aceptación: 25/02/2025

Fecha de Publicación: 04/04/2025

PAG: 1-18

Abstract

This paper examines the performance of IPE perforated shear connectors, emphasizing their role in maintaining the structural integrity of composite beams. It focuses on inspecting the behavior of these connectors under pull-out forces to assess their resistance capabilities and conformity with Eurocode 4 guidelines. Pull-out tests were conducted to evaluate whether the perforated IPE connectors meet Eurocode 4's requirement of providing a minimum resistance equivalent to 10% of the shear strength. Simultaneously, the study explores two crucial parameters: hole shapes (encompassing circular and long cut holes) and the diameters of perforating steel rebar (6 mm and 8 mm) key outcomes center on comprehending load-separation curves, illustrating the connectors' performance across varied conditions. Additionally, a meticulous examination and analysis of failure modes were undertaken to interpret and derive meaningful insights from the results. Furthermore, the study employs finite element simulations using the 3D code Abaqus to analyze the behavior of IPE perforated connectors under pull-out conditions, particularly emphasizing the role of anti-uplift rebar passing through perforated holes. Remarkably, the findings conclusively affirm the effectiveness of IPE perforated connectors in withstanding pull-out forces, exceeding the prescribed 10% threshold of shear resistance under tensile stresses as mandated by Eurocode standards.

Keywords: Composites beams; IPE perforated connector; Pull-out strength; load-separation curves; Failure modes; Pull-out test; 3D finite element code; pullout forces.

Resumen

Este artículo examina el desempeño de los conectores perforados de esfuerzo cortante IPE, haciendo hincapié en su papel en el mantenimiento de la integridad estructural de las vigas compuestas. Se centra en inspeccionar el comportamiento de estos conectores bajo fuerzas de extracción para evaluar sus capacidades de resistencia y conformidad con las directrices del Eurocódigo 4. Se realizaron pruebas de extracción para evaluar si los conectores perforados de IPE cumplen con el requisito del Eurocódigo 4 de proporcionar una resistencia mínima equivalente al 10% de la resistencia al corte. De forma simultánea, el estudio explora dos parámetros cruciales: formas de los orificios (que abarcan orificios de corte circulares y largos) y los diámetros de las barras de refuerzo de acero perforadas (6 mm y 8 mm). Los resultados clave se centran en comprender las curvas de separación de carga, que ilustran el desempeño de los conectores en diversas condiciones. Adicionalmente, se realizó un examen y análisis meticuloso de los modos de falla para interpretar y derivar información significativa de los resultados. Más aún, el estudio emplea simulaciones de elementos finitos utilizando el código 3D Abaqus para analizar el comportamiento de los conectores perforados IPE en condiciones de extracción, haciendo hincapié en el papel de las barras de refuerzo anti-elevación que pasan a través de los agujeros perforados. Cabe destacar que los hallazgos afirman de manera concluyente la eficacia de los conectores perforados IPE para soportar fuerzas de extracción, superando el umbral prescrito del 10% de resistencia al corte bajo tensiones de tracción, tal como lo exigen las normas del Eurocódigo.

Keywords: Vigas compuestas; conector perforado IPE; resistencia a la extracción; curvas de separación de carga; modos de falla; prueba de extracción; código de elementos finitos 3D; fuerzas de extracción.

Corresponding author: farid.boursas@univ-tebessa.dz

Department of Civil Engineering, University of Larbi Tébessi Tébessa, Laboratoire de Génie Civil appliqué, Algeria

1. Introduction

The structural integrity of composite beams, specifically the separation between concrete slabs and steel beams in pullout conditions, has seen limited exploration in research. Early observations of the uplift phenomenon by Chapman and Balakrishnan, (1964) highlighted its presence during experimental studies on isostatic composite beams. Aribert, (1997) integrated potential steel and concrete separation into calculations for composite beams, noting a low uplift/sliding ratio in angle connectors. Recent studies have focused on shear connector behaviours under tension loading (Aribert, 2004). Yu et al., (2012) utilized a 3D numerical model to simulate Perforated connectors' Pullout and Pushout tests, emphasizing concrete strength's role in elasticity bearing capacity and perforating rebar's role in ultimate bearing capacity. Kim et al., (2016) explored Pullout resistance in ten perforated shear connector specimens, investigating parameters like connector length and perforating rebar characteristics. A tested steel-concrete composite beam with pre-damage through pullout tests and subsequent pushout tests establishes a predictive numerical model for combined shear and tension loading (Heng et al., 2017). Research on demountable connectors observed reduced shear resistance under pullout loads (Tan et al., 2019), while Zheng et al., (2019) introduced notched hole shapes for perforated connectors, highlighting their practicality and efficiency. Xu et al., (2022) developed a numerical model to simulate corrosion-induced damage in headed studs, enabling the prediction of strength reduction factors.

Various studies focused on optimizing I-shaped and T-shaped perforated connectors to enhance assembly, fixability, and economic feasibility. Vianna et al., (2008) conducted a parametric study on T-shaped perforated connectors, evaluating parameters like slab concrete thickness, compressive strength, connector geometry, position concerning shear load, and hole arrangement. The same authors carried out a comparative analysis of perforated plates and T-shaped perforated connectors (Vianna et al., 2009). Ahn et al., (2010) modified shear strength equations considering the involvement of perforated plates. Costa-Neves et al., (2013) tested innovative I-shaped and 2T-shaped perforated connectors, comparing experimental results with analytical models. Maghaghi et al., (2021) investigated channel connectors under pushout and pullout tests, observing stress concentration and plastic hinge formation. Farid and Boutagouga, (2021) performed a parametric study on the IPE connector's orientation, revealing optimal configurations for increased shear strength and minimum vertical separation resistance.

Eurocode 4 (Standardization, 1994) mandates that shear connectors must resist at least 10% of the ultimate shear strength to prevent tearing. This study aims to enhance the resistance of perforated IPE connectors by examining configurations with circular and long-cut holes intersected by 6mm and 8mm diameter steel bars. The findings provide new insights into optimizing connector design to improve structural performance and prevent tearing, contributing to more effective guidelines for composite girders.

2. Experimental procedure

This paper's primary focus is on examining IPE perforated steel shear connectors subjected to pull-out forces. These connectors, depicted in (Figure 1), feature perforations with circular and long cut holes through which steel rebar passes. Additionally, the study aims to analyze the behaviour of connectors with these two-hole types, drawing comparisons in terms of pull-out strength, ductility, and failure mode.



Figure 1. IPE perforated shear connectors studied.

2.1 Specimens preparation

In this research, the composite beam comprises a concrete slab ($36 \times 32 \times 12 \text{ cm}^3$) reinforced by $4\Phi 8$ reinforcement in both directions. The study involves four specimens investigated in a pullout test. These specimens include IPE6C, featuring IPE80 with a circular hole and a passing rebar diameter of 6mm; IPE8C, consisting of IPE80 with a circular hole and a passing rebar diameter of 8mm; IPE6N, employing IPE80 with a long cut hole and a passing rebar diameter of 6mm; and finally, IPE8N, utilizing IPE80 with a long cut hole and a passing rebar diameter of 8mm. The IPE80 perforated connectors were affixed to a 15 mm thick steel plate with a diameter of 100 mm and welded onto 48 mm nuts using two elongated steel plates. The Shielded Metal Arc Welding (SMAW) process uses E6013 rutile electrodes. This setup was designed to prevent direct contact between the concrete, nuts, and the 15 mm steel plate, as illustrated in (Figure 2).



Figure 2. Preparing device of the testing connector.

The pull-out specimens were arranged to be poured in an inverted position, ensuring the placement of the connectors at the concrete slab's center. Notably, the steel plate and nut were positioned to avoid submersion in concrete, as depicted in (Figure 3).



Figure 3. Concrete pouring of specimens.

2.2 Material properties

2.2.1 Steel

A specimen from the IPE80 web is used for standard tensile testing to establish the connector's stress-strain curve. The specimen's dimensions comply with (ISO 6892-1, 2011).

(Table 1) presents the material properties obtained from these tests, such as yield stress, and ultimate tensile stress for the IPE80 connector.

Table 1. Mechanical properties of the connector steel.

Type	f_y (MPa)	f_u (MPa)
IPE80	238	358

2.2.2 Concrete

Four cylindrical concrete samples measuring 160 mm in diameter and 320 mm in height were cast using the concrete mix. These specimens underwent uniaxial compressive strength testing on the same day as the pull-out tests after being cured by immersion in a water basin. Concrete cylinders were tested at 28 days, and the results of these concrete compressive tests are displayed in (Table 2).

Table 2. Compressive strength of concrete.

F_{c28} (Mpa)	average F_{c28} (Mpa)
30.453	30,454
30.289	
29.866	
31.208	

3. Test setup and loading procedure

A steel frame was constructed using HEB beams. In the lower beam, a 40 mm diameter nut was welded, and it housed a threaded rod of the same diameter. A steel chair was also fabricated to support the pull-out specimens, as illustrated in (Figure 4).

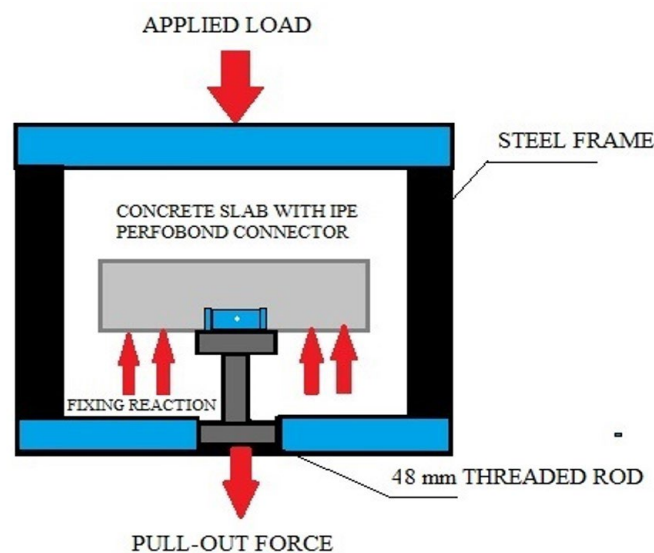


Figure 4. Pull-out mechanism.

A concentrated, steady force is exerted at the central top of the steel frame, initiating a pull-out action on the connector. This force is applied using a precisely calibrated hydraulic jack connected to an electric hydraulic pump with a 500 kN capacity. To track the separation between the connector and the concrete slab, a linear variable differential transformer (LVDT) is utilized. This LVDT is linked to a data acquisition system

positioned at the steel frame's top center, enabling the measurement of the total displacement throughout the pull-out test, as illustrated in (Figure 5). The test procedure follows the guidelines outlined in B.2.4 Testing Procedure of Eurocode 4 (Standardization, 1994). The load is incrementally increased from 0 to 8 kN (40% of the expected failure load) in 1 kN steps before being reduced to 2 kN (5% of the expected failure load). This cycle, ranging between 2 kN and 8 kN, is repeated 25 times to eliminate any discrepancies in the setup. Subsequently, the applied load is continuously increased until the point of failure.



Figure 5. Test setup.

4. Experimental Results

The pull-out test was employed to examine the performance of IPE perforated shear connectors within composite girders. This study aimed to scrutinize the load separation behaviour, assess the ultimate pull-out capacity, and discern the various failure modes exhibited by the IPE perforated connectors. In this context, separation refers to the vertical displacement measured between the steel beam and the concrete slab, which is represented by the displacement of the connector.

4.1 "I" shaped perforated connectors with a circular hole

The initial experimental tests investigated the response of IPE perforated shear connectors with circular holes to tensile forces. The specimens were categorized as IPE6C, indicating those with a 6 mm diameter anti-lift rebar, and IPE8C, representing specimens with an 8 mm diameter anti-lift rebar. The load separation curves for these tested IPE perforated connectors with circular holes are depicted in (Figure 6).

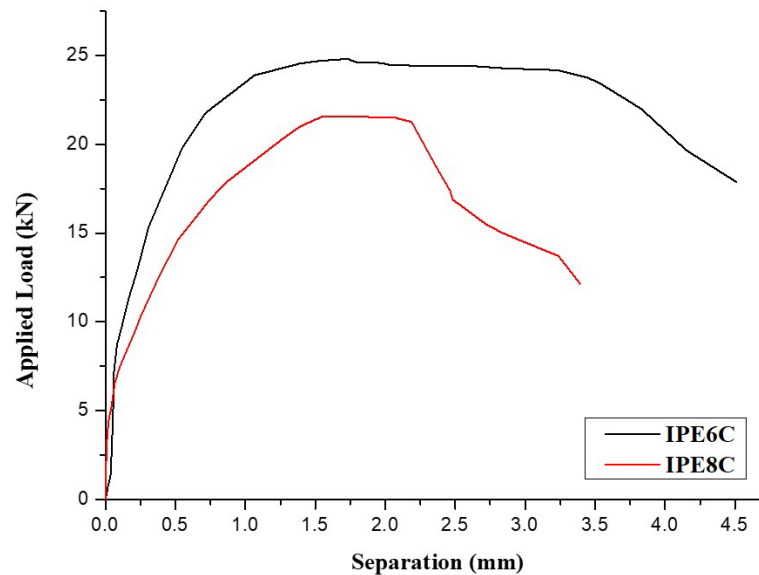


Figure 6. Load-separation curve of IPE80 connectors with 6 mm and 8mm dia of rebar and a circular hole.

The observations highlight the behavior of both IPE6C and IPE8C perforated connectors, as depicted in (Figure 6). Notably, the IPE6C connectors display slightly superior strength compared to their IPE8C counterparts. Failures occurred at separations measuring 4.5 mm for IPE6C and 3.50 mm for IPE8C. The diameter of the anti-lift rebar significantly influences pullout resistance, with larger rebar diameters leading to decreased separation capacity in perforated connectors. Specifically, IPE8C and IPE6C failed at maximum loads of 21.53 kN and 24.79 kN per connector, respectively.

At an initial load of 11,5 kN per connector, initial cracks emerged on the outer surfaces of the concrete slabs. In the case of IPE6C, where a 6 mm diameter anti-lift rebar was used, these cracks did not deeply penetrate the concrete slabs. This configuration effectively delayed concrete slab failure. However, when employing an 8 mm diameter anti-lift rebar (IPE8C), the concrete experienced brittle failure, accelerating crack propagation. Across all perforated connectors with circular holes, the failure mode consistently involved concrete cracking and subsequent crushing, forming the distinctive concrete cone observed in (Figure 7).



Figure 7. Failure of specimens IPE6C, IPE8C.

4.2 "I" shaped perforated connectors with a long cut hole

In the ensuing experimental tests, we investigated the performance of IPE perforated connectors incorporating an elongated cut hole (see (Figure 1b)). The objective of this examination was to understand the influence of hole shape on pullout capacity, failure modes, and load separation behavior. The specimens under investigation were designated as follows: IPE6N denoting those featuring a 6 mm diameter anti-lift rebar, and IPE8N representing specimens equipped with an 8 mm diameter anti-lift rebar.

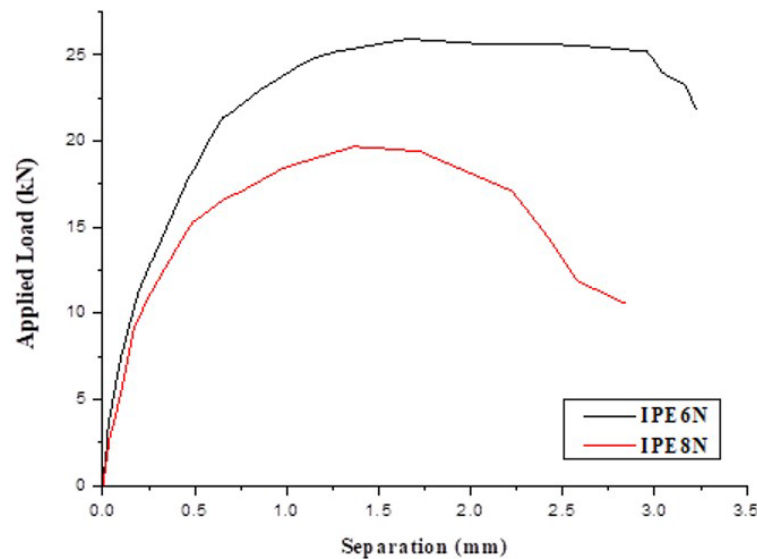


Figure 8. Load-separation curve of IPE80 connectors with 6 mm and 8mm dia of rebar and long cut hole.

As depicted in (Figure 8), the IPE8N and IPE6N connectors demonstrated ultimate pullout capacities of 19.67 kN and 25.91 kN per connector, respectively, while their ultimate separation capacities reached 3.22 mm and 2.84 mm.

In all instances of the perforated connectors featuring a long cut hole, the failure mode was consistent, characterized by concrete cracking and subsequent crushing. Early cracks were visible on the concrete slab surfaces, originating around the connector positioned centrally within the slab at an approximate load of 10,5 kN per connector. These cracks are attributed to the perforating rebar and the concrete slab's strength, as highlighted in (Figure 9).



Figure 9. Concrete failure for IPE6N, IPE8N.

5. Comparison between shear resistance and pullout resistance of IPE perforated connectors

According to Annex B of Eurocode 4, the behaviour of perforated IPE shear connectors in composite girders was examined through push-out tests. These tests were performed on connectors with the same dimensions, reinforcement, and material properties as those used in the pull-out tests. The study investigates their load-slip behaviour under shear conditions, with the test arrangement and procedure detailed by (Boursas et al., 2024).

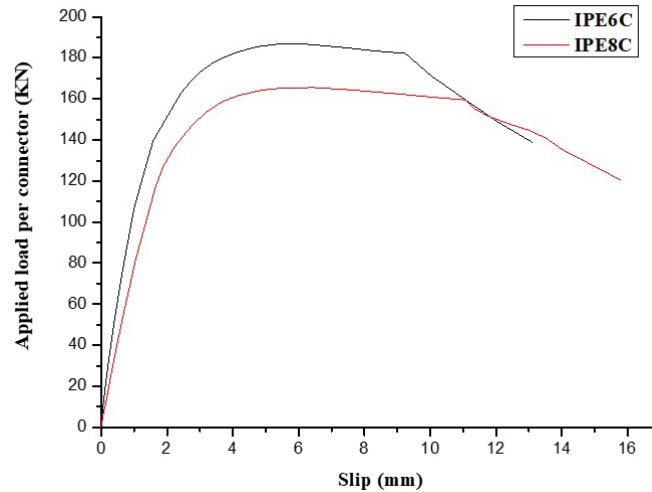


Figure 10. Push-out test results for IPE80 with a circular hole.

The diameter of the anti-lift rebar significantly influences the shear resistance; we note that the load capacity of perforated connectors decreases by increasing the anti-lift rebar diameter. (Figure 10) illustrates that IPE6C and IPE8C failed at the maximum loads of 186.92 kN and 165.52 kN per shear connector, respectively.

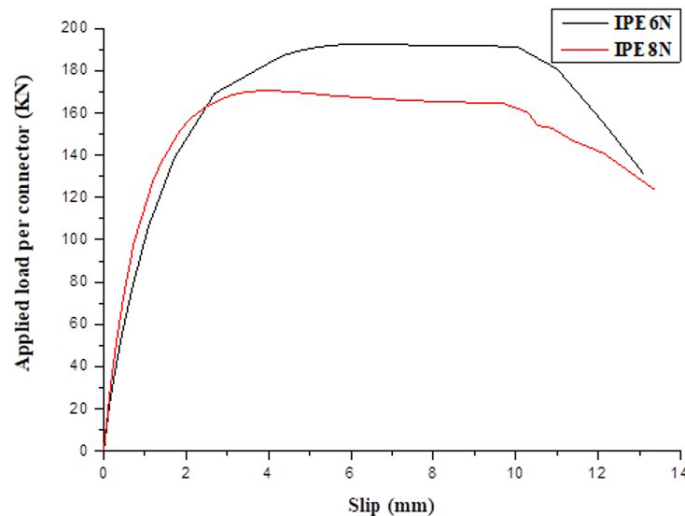


Figure 11. Push-out test results for IPE80 with long cut-hole.

As shown in (Figure 11), the ultimate shear capacities recorded were 192.65 kN and 170.70 kN per connector for IPE6N and IPE8N, where the ultimate slip capacities were 13.26 mm and 16.72 mm, respectively.

Respecting the Eurocode specifications, a comparison between the ultimate load of pull-out tests and the shear resistance of the IPE perforated is shown in (Table 3).

Table 3. Comparison between Pullout and Pushout tests.

Studied connectors	Pull-out ultimate load (kN)	Push-out ultimate load (kN)	Comparison pull-out/push-out
IPE6C	24.22	186.92	12.96%
IPE8C	22.07	165.52	13.33%
IPE6N	25.16	192.65	13.06%
IPE8N	19.93	170.7	11.68%

According to the data presented in (Table 3), the pullout strength-to-shear strength ratio for the examined connector types surpassed the Eurocode 4 recommended threshold of 10%. In our specific study, we observed ratios of 13.29% for IPE6C, 13.24% for IPE8C, 13.06% for IPE6N, and 11.68% for IPE8N.

6. Numerical modelling of pullout test

6.1 Element type and mesh

The three-dimensional C3D8R eight-node solid brick elements with reduced integration are adopted to mesh the concrete slab generating 3830 elements, the IPE80 shear connector and the anti-lifting rebar. A two-node T3D2 mesh element is used for reinforcing rebars. The truss element in Abaqus, (2011) can be used in two or three dimensions to present a thin structural element that resists and transfers only axial forces. It can also be used to model components where deformation is calculated from the change in length. The advantage of using a truss element is that the perfect bond can easily be defined by embedding the steel bars in a host region (concrete slab in our case, as illustrated in (Figure 12)).

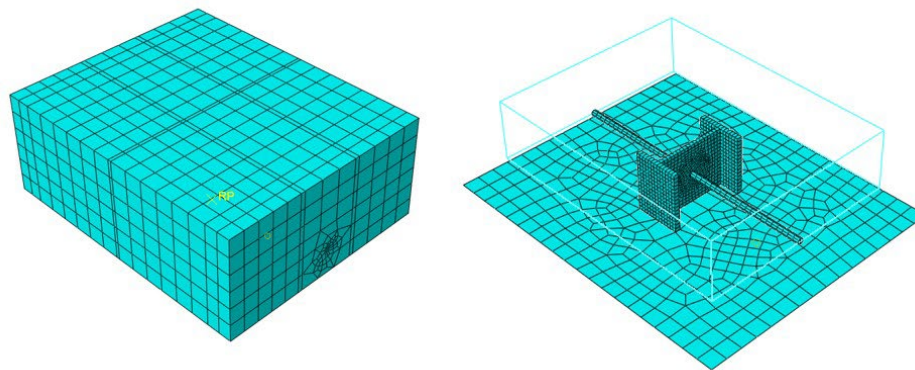


Figure 12. Finite element mesh of the specimen.

6.2 Material Modeling

(Figure 13) depicts the nonlinear stress-strain characteristics of concrete under compression and tension. The Concrete Damage Plasticity model from the ABAQUS material library was employed. This particular material model is suitable for simulating the failure of concrete with similar degradation patterns. In our simulation, the material dilation angle was set to 31, and an eccentricity value of 0.1 was utilized. Moreover, a ratio of 1.16 between biaxial compressive strength and uniaxial compressive strength was adopted, while the tensile-to-compressive meridian ratio was established as 0.667 (Hafezolzghorani et al., 2017). A simplified bi-linear stress-strain behavior is adopted for steel reinforcement and I-connectors, as shown in (Figure 14).

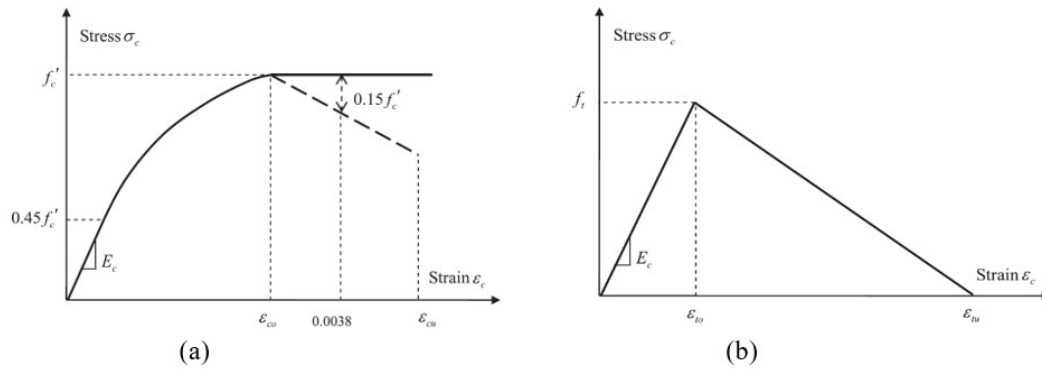


Figure 13. Finite element mesh of the specimen.

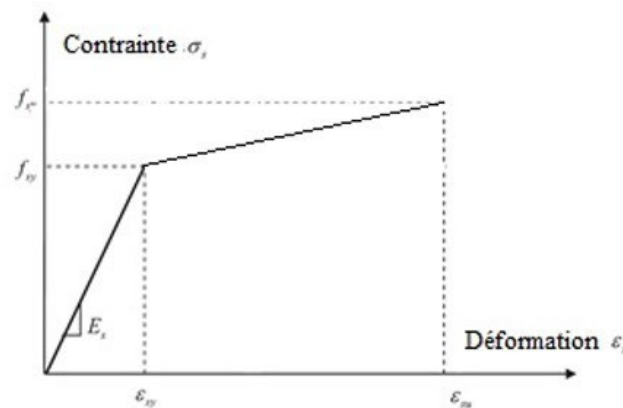


Figure 14. Finite element mesh of the specimen.

6.2 Interactions and loading

The contact pair method is used to define the “surface to surface” contact between the concrete slab, IPE80 perforated shear connectors, and rebar. In experimental pull-out tests, the surface of the rigid base in contact with the concrete slab is generally greased to reduce friction. In our FE model, frictionless contact interaction was applied to the surfaces of the rigid base and concrete slab.

A tangential interaction was used for the interface of the I-shaped connector and the reinforced concrete slab; the coefficient of friction was taken at 0.20. Reinforcing bars are located inside the concrete slab, as shown in (Figure 15). Integrated stress (embedded constraint) applied to rebar and slab.

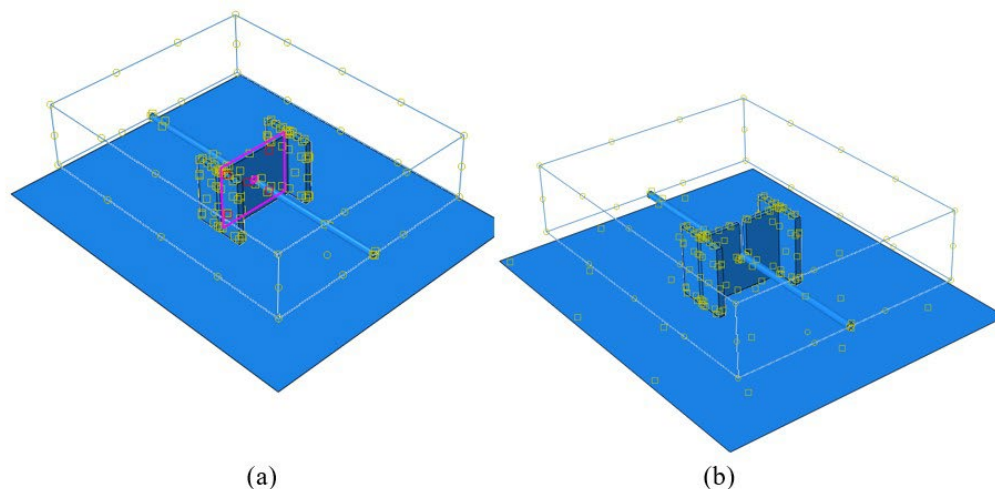


Figure 15. Interaction and constrain conditions of the specimen.

All six degrees of freedom (three translational and three rotational) of the rigid base reference node are restricted. In this analysis, an imposed displacement is applied to the lower surface of the IPE80 perforated shear connectors, as shown in (Figure 16).

The separation was measured as the relative displacement between IPE80 shear connector nodes. The load was measured as the total reaction acting on the loading surface.

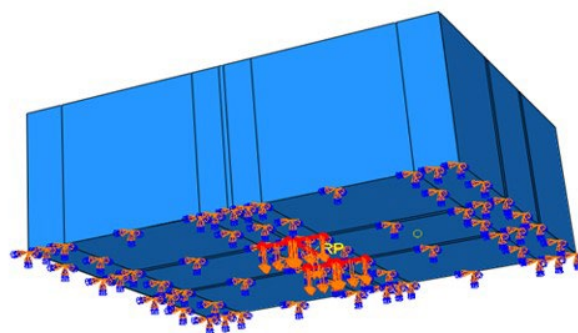


Figure 16. Loading of the specimen.

7. Models validation

The numerical results obtained were compared with the results of the experimental tests. The comparison in (Figure 17) and (Figure 18) show that the 3D finite element model established during this study is capable of effectively predicting pullout strength and load-separation curve for pullout tests with perforated IPE80 connectors.

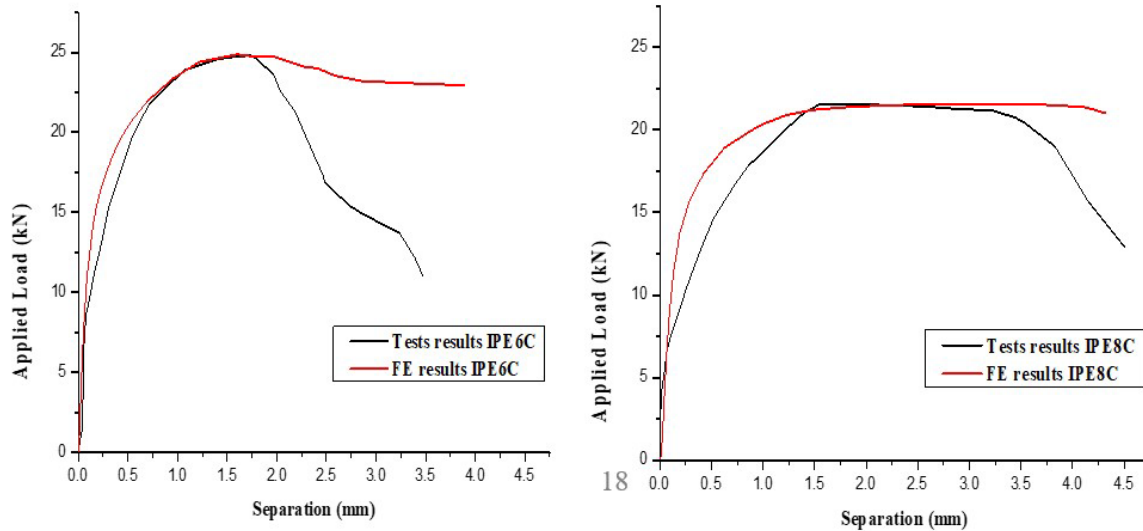


Figure 17. Load-separation curve of IPE80 connector with a circular hole.

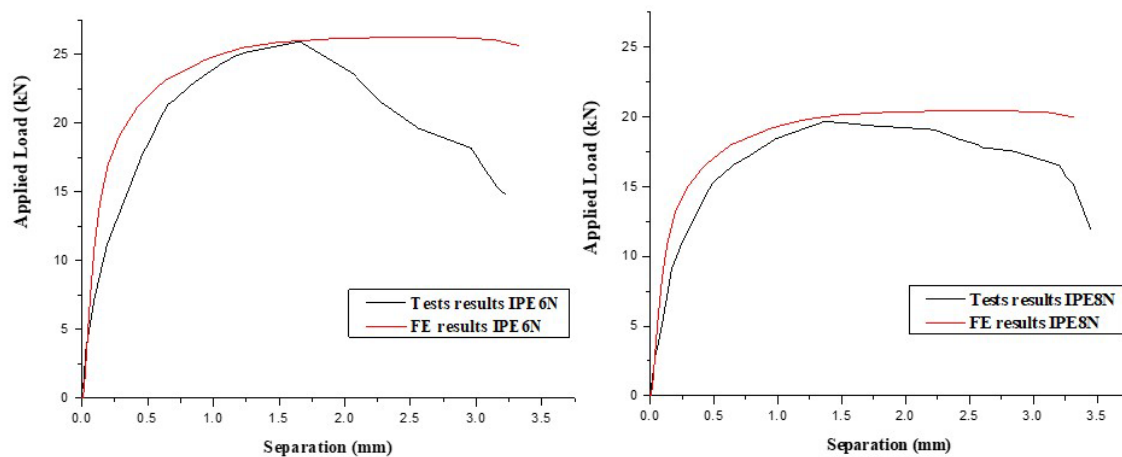


Figure 18. Load-separation curve of IPE80 connector with long cut hole.

Increasing the diameter of the holes and the rebar passing through them from 6 mm to 8 mm resulted in a decrease in the pullout resistance of the perforated IPE80 shear connector by 12%. These findings indicate that enlarging the hole diameter negatively impacts the connector's resistance to pull out. The primary reason for this is that the failure mode is dependent on the concrete failure within the hole, and the strength decreases as the hole diameter increases.

(Figure 19) illustrates an observable expansion of the IPE holes under investigation, indicating stress concentration around these openings prior to the reinforced concrete slab failure. This phenomenon is evident in both circular and long-cut forms of the holes. Subsequently, a deformation in the form of local buckling is observed, particularly in the case of circular holes. This issue is alleviated by employing holes with a long cut. Considering the ease of utilizing long-cut IPE connectors and their nearly identical tensile strength compared to connectors with circular holes, it is advisable to prefer long-cut connectors over their circular-hole counterparts.

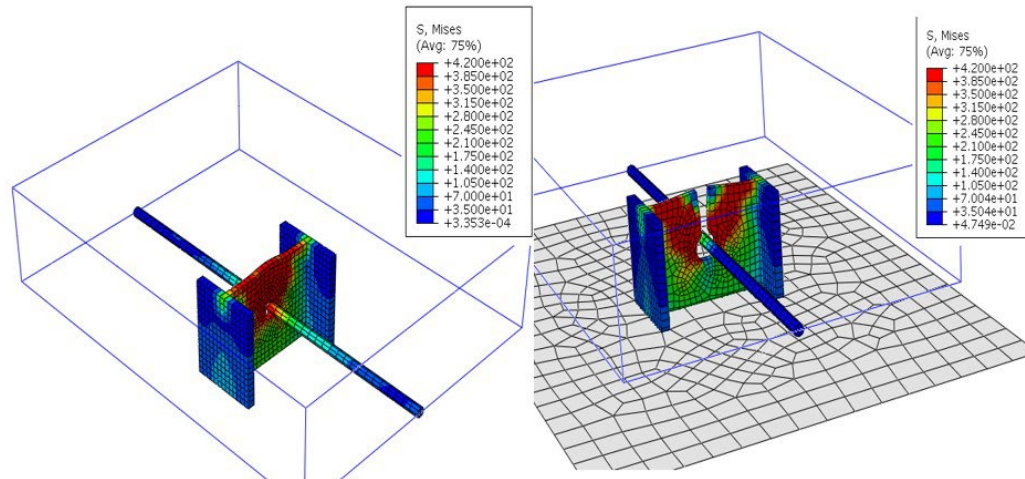


Figure 19. Stress distribution in IPE80 perforated connectors.

8. Parametric study on IPE connectors with long cut hole

The parameters chosen for this parametric study were determined based on prior research (Boursas, 2022); (Koaik et al., 2016), which highlighted their substantial impact on the tensile resistance of connectors. We selected the most pertinent parameters to analyze their influence on pullout resistance. These include the concrete strength, connector grade, reinforcing bar strength, IPE hole and reinforcement diameter. Concrete strength is crucial since it directly impacts the overall structural strength (Rezaeian et al., 2024). Connector grade and reinforcing bar strength are equally significant, influencing the connectors' strength and load transfer capacity (Kim et al., 2017). Furthermore, the diameter of IPE holes and rebars are vital parameters affecting the connectors' load transfer capacity and pullout resistance (Gascon, 2016); (Jiang et al., 2021). Assessing the impact of each parameter on pullout resistance allows for a better understanding of how these factors contribute to connector performance under diverse conditions (Huang et al., 2024).

8.1 Influence of concrete strength

The impact of variations in concrete strength on the tensile behavior of perforated shear connectors was studied, as depicted in (Figure 20).

(Figure 20) illustrates the impact of concrete strength on the behaviour of perforated shear connectors under tensile loading. An increase in concrete strength from 30 MPa to 40 MPa and 50 MPa resulted in respective increases in tearing strength of 21% and 28%. This study demonstrates that an increase in concrete strength significantly improves the tear resistance of perforated IPE connectors. This improvement can be attributed to the reduction of the damaged area of the concrete under tensile. Therefore, the use of higher-strength concrete can enhance the tear resistance of the perforated shear connector. However, when the strength of the concrete exceeds 40 MPa, the pull-out resistance tends not to increase. This may be because reinforcing bars are required to match the higher concrete strength to achieve the total concrete strength.

8.2 The Influence of the Steel Grade of the IPE80 Perforated Connector

According to (Figure 21), the steel grade of the Perforated IPE80 connector has a significant impact on tensile behaviour. When the tensile force of the perforated connector is S235 steel, the tensile strength is 21.71 kN. In comparison, the S275 and S355 steel connectors supported tensile forces of 25 kN and 32 kN, respectively, indicating higher strength compared to S235 steel perforated connectors.

The results indicate that increasing the grade of the perforated connector leads to an increase in the tear strength of the perforated IPE80 shear connector. Therefore, using a higher grade can improve the tear resistance of the notched perforated shear connector.

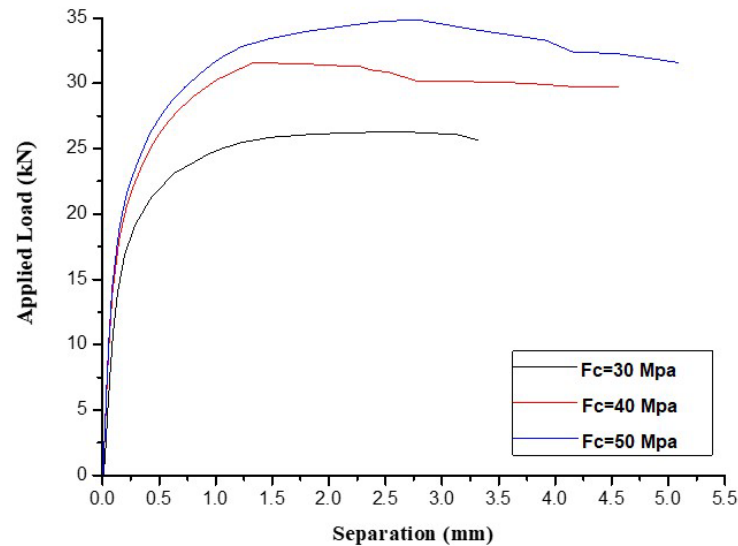


Figure 20. Influence of concrete compressive strength.

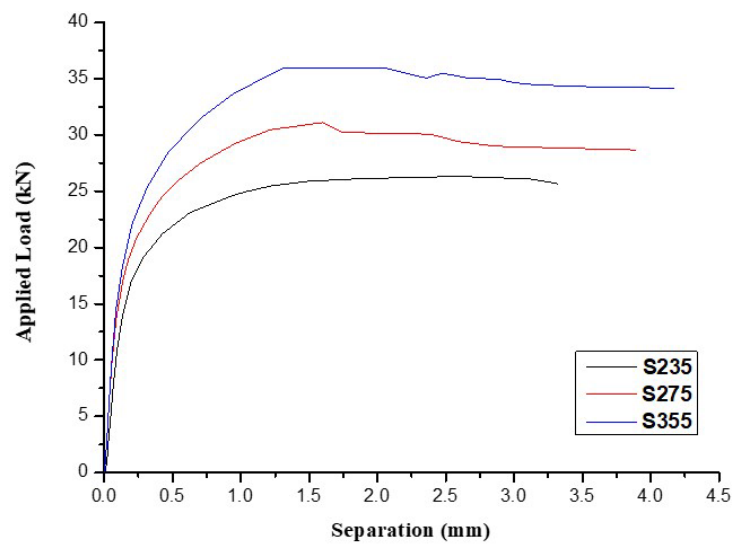


Figure 21. Influence of IPE80 steel grade.

8.3 The Influence of Rebar Strength

When the yield strength of the reinforcing bar was increased from 335 MPa to 400 MPa and 500 MPa, the tear resistance of the perforated IPE80 connector increased by 14% and 15%, respectively, as shown in (Figure 22). These results suggest that the increase in the strength of the reinforcement leads to an improvement in the tear resistance of the perforated shear connector. A possible explanation for this observation is that using a more robust reinforcing bar in the hole enhances the combined effects of the reinforcing bar and concrete in the hole. However, the results also showed that when the yield strength of the reinforcing bar exceeded 400 MPa, the tear resistance tended not to increase. This observation may be due to the need for stronger concrete to achieve the full strength of the perforating reinforcement in the hole, aligning with the high-strength reinforcing bar. Finally, these results emphasize the importance of reinforcement strength in enhancing the tear resistance of perforated shear connectors, highlighting the need to find the optimal combination between reinforcement strength and concrete strength to achieve maximum pull-out strength.

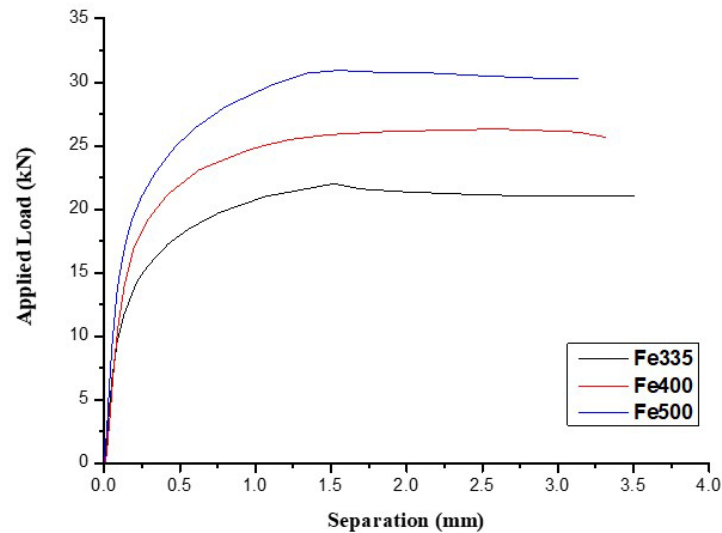


Figure 22. Influence of reinforcement strength.

8.4 The Influence of Hole Diameter and Rebar Passing Through the Hole

The impact of the hole diameter and the diameter of the reinforcing bar passing through the hole on the tear behavior of perforated shear connectors is illustrated in (Figure 23).

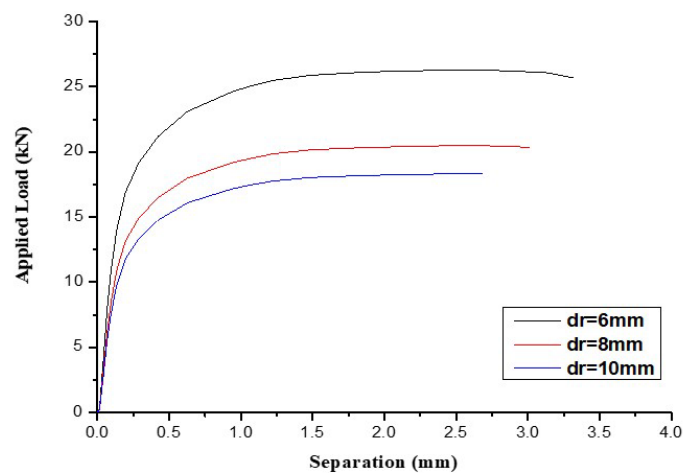


Figure 23. Influence of hole diameter and rebar passing through the hole.

An increase in the diameter of the holes and the rebar passing through the hole from 6 mm to 8 mm and 10 mm resulted in respective decreases of 2% and 12% in the tear resistance of the perforated IPE80 shear connector. The results indicate that increasing the diameter of the hole from 6 mm to 10 mm negatively affected the tear resistance of the connector. The main reason is that the failure mode depends on the concrete shear in the hole, the strength of which decreases with the increase in the diameter of the hole. However, even with a hole diameter of 8 mm, the decrease in tear resistance tends to be smaller. A decrease in the perforation reinforcement's holding effect on the hole concrete could explain this trend.

9. Conclusion

This study examined the tensile resistance of composite beams and the importance of shear connectors, highlighting the need to select suitable connectors according to the specific requirements of the structure. Pullout and push-out tests were conducted to explore the tensile strength, ductility, and stiffness of IPE perforated shear connectors in composite slabs. The following key findings emerge from the experimental study:

- The hole shape of the IPE perfobond connector did not significantly impact pullout ultimate load capacity and ductility.
- The long cut-hole shape of the IPE perforated connector outperforms the circular hole in terms of ultimate load capacity and ease of implementation.
- Pullout strength decreases by approximately 10% with a 6 mm to 8 mm increase in the diameter of the passing rebar in circular holes and about 22% for long-cut holes.
- Failure modes observed for all studied IPE perfobond connectors involve crushing a concrete cone.
- The passing rebar plays a crucial role, especially in resisting uplift, ensuring the 10% shear capacity in the pullout recommended by Eurocode 4.
- The hole geometry of the IPE perfobond shear connector significantly influences shear load capacity and ductility, with the long cut-hole shape excelling in shear resistance but less effective in interfacial slip compared to the circular hole.
- IPE perfobond shear connectors tested in push-out tests exhibit sufficient ductility in the studied hole shapes.
- Shear capacity decreases by approximately 12% with an increase in the diameter of the passing rebar from 6 mm to 8 mm for both types of holes studied. However, there is a gain in ductility of about 25%.
- The perforating rebar, crucial for resistance to uplift as recommended by Eurocode 4, also contributes to the shear resistance of the composite slab, in accordance with Section 6.6.1.1 (7)P and (8), which requires shear connectors to prevent separation of the concrete from the steel element and to resist a nominal ultimate tensile force perpendicular to the steel flange.
- Stress concentration at the hole in perforated IPE connectors was also noted, highlighting the importance of considering mechanical strength differences between the anti-slip bar and the perforated IPE and the relatively thin thickness of the IPE to minimize undesirable deformations.
- The parametric study revealed key factors influencing the tensile resistance of perforated IPE connectors. Results indicated that increasing concrete strength, employing higher-grade steel for connectors, enhancing rebar strength, and increasing hole diameter all contributed to improved pullout resistance. These findings provide valuable insights for optimizing the design and performance of perforated IPE connectors.

10. Acknowledgments

This research was supported by Algeria's Directorate-General for Scientific Research and Technological Development (DGRSDT). A special thank you to the University of Larbi Tebessi and the laboratory of applied civil engineering. Any opinions, findings, conclusions, or recommendations expressed in this publication are those of the authors.

11. Notes on Contributors

F. Boursas, Department of Civil Engineering, University of Larbi Tébessi Tébessa, Laboratoire de Génie Civil appliqué, Algeria.
ORCID <https://orcid.org/0000-0001-6491-4205>

B. Maghaghi, Civil Engineering Department, Ferhat Abbas-setif1 University, Setif 19000, Algeria
ORCID <https://orcid.org/0000-0003-1282-1140>

R. Boufarh, Department of Civil Engineering, University of Larbi Tébessi Tébessa, Laboratoire de Génie Civil appliqué, Algeria.
ORCID <https://orcid.org/0000-0002-1793-2950>

M. Saidani, School of Energy, Construction and Environment, Coventry University, Coventry, UK
ORCID <https://orcid.org/0000-0002-5861-676X>

12. References

- Abaqus, G. (2011).** Dassault Systemes Simulia Corporation, . Providence, RI, USA.
- Ahn, J.-H.; Lee, C.-G.; Won, J.-H.; Kim, S.-H. (2010).** Shear resistance of the perfbond-rib shear connector depending on concrete strength and rib arrangement. *Journal of Constructional Steel Research*, 66(10), 1295-1307. <https://doi.org/10.1016/j.jcsr.2010.04.008>
- Aribert, J.-M. (1997).** Analyse et formulation pratique de l'influence de la nuance de l'acier du profilé sur le degré minimum de connexion partielle d'une poutre mixte. *Construction Métallique* (3).
- Aribert, J.-M. (2004).** Construction mixte acier-béton-Calcul des poutres mixtes. *Les superstructures du bâtiment*. <https://doi.org/10.51257/a-v1-c2561>
- Boursas, F. (2022).** Analyse du comportement de la connexion dans les poutres composites acier-béton: Modélisation numérique et étude paramétrique [University of Larbi Tébessi Tébessa].
- Boursas, F.; Boufarh, R.; Sifeddine, A. (2024).** Experimental investigation on the shear resistance of I-shaped perforated connectors in composite beams. *Architecture and Engineering*, 9(3), 39-52. <https://doi.org/10.23968/2500-0055-2024-9-3-39-52>
- Chapman, J.; Balakrishnan, S. (1964).** Experiments on composite beams. *The Structural Engineer*, 42(11), 369-383.
- Costa-Neves, L. F.; Figueiredo, J. P.; Vellasco, P. C. G. d. S.; Vianna, J. d. C. (2013).** Perforated shear connectors on composite girders under monotonic loading: An experimental approach. *Engineering Structures*, 56, 721-737. <https://doi.org/10.1016/j.engstruct.2013.06.004>
- Farid, B.; Boutagouga, D. (2021).** Parametric study of I-shaped shear connectors with different orientations in push-out test. *Fracture Structural Integrity*, 15(57), 24-39. <https://doi.org/10.3221/igf-esis.57.03>
- Gascon, M. (2016).** Étude du comportement de connecteurs de cisaillement dans du béton fibré à ultra-hautes performances pour la construction de poutres mixtes de ponts [École Polytechnique de Montréal]. <https://publications.polymtl.ca/2133/>
- Hafezoghforani, M.; Hejazi, F.; Vaghei, R.; Jaafar, M. S. B.; Karimzade, K. (2017).** Simplified damage plasticity model for concrete. *Structural engineering international*, 27(1), 68-78. <https://doi.org/10.2749/101686616x1081>
- Heng, P.; Bud, M.; Somja, H.; Hjjaj, M.; Battini, J.-M. (2017).** Residual stiffness and strength of shear connectors in steel-concrete composite beams after being subjected to a pull-out pre-damaging: An experimental investigation. *Structures*, 11, 189-205. <https://doi.org/10.1016/j.istruc.2017.05.003>
- Huang, W.; Zhan, Y.; Zhang, C.; Lyu, W.; Li, Y.; Shao, J. (2024).** Tensile resistance and shear-tension interaction relationship of T-type perfbond rib shear connectors. *Journal of Building Engineering*, 89, 109183. <https://doi.org/10.1016/j.jobbe.2024.109183>
- ISO, 6892-1. (2011).** tensile testing: initial experience from the practical implementation of the new standard. 53(10), 595-603.
- Jiang, H.; Fang, H.; Liu, J.; Fang, Z.; Zhang, J. (2021).** Experimental investigation on shear performance of transverse angle shear connectors. *Structures*, 33, 2050-2060. <https://doi.org/10.1016/j.istruc.2021.05.071>
- Kim, S.-H.; Kim, K.-S.; Lee, D.-H.; Park, J.-S.; Han, O. (2017).** Analysis of the shear behavior of stubby Y-type perfbond rib shear connectors for a composite frame structure. *Materials*, 10(11), 1340. <https://doi.org/10.3390/ma10111340>
- Kim, Y.-H.; Kang, J.-Y.; Koo, H.-B.; Kim, D.-J. (2016).** Pull-Out Resistance Capacity of a New Perfbond Shear Connector for Steel Pile Cap Strengthening. *Advances in Materials Science Engineering*, 2016(1), 1374689. <https://doi.org/10.1155/2016/1374689>
- Koalk, A.; Alachek, I.; Reboul, N.; Bel, S.; Jurkiewicz, B. (2016).** Caractérisation du collage béton-béton par essais push-out. *Academic Journal of Civil Engineering*, 34(1), 126-133.
- Maghaghi, B.; Titoum, M.; Mazoz, A. (2021).** Experimental evaluation of new channel shear connector shapes. *International Journal of Steel Structures*, 21(3), 883-900. <https://doi.org/10.1007/s13296-021-00478-x>
- Rezaeian, A.; Mansoori, M.; Khajehdezfuly, A. (2024).** Performance of steel beam with welded top-seat angle connections at elevated temperatures. *Journal of Structural Fire Engineering*, 15(1), 113-146. <https://doi.org/10.1108/jsfe-07-2022-0026>
- Standard, B. (1993).** Eurocode 3. Design of steel structures. In BS EN (Vol. 1, pp. 2005).
- Standard, B. (2004).** Eurocode 2. Design of concrete structures. In Part (Vol. 1, pp. 230).
- Standardization, E. C. f. (1994).** Design of composite steel and concrete structures. Part 1-1: General rules and rules for buildings. In Eurocode.
- Tan, E. L.; Varsani, H.; Liao, F. (2019).** Experimental study on demountable steel-concrete connectors subjected to combined shear and tension. *Engineering Structures*, 183, 110-123. <https://doi.org/10.1016/j.engstruct.2018.12.088>
- Vianna, J. d. C.; Costa-Neves, L.; Vellasco, P. d. S.; De Andrade, S. (2008).** Structural behaviour of T-Perfbond shear connectors in composite girders: An experimental approach. *Engineering Structures*, 30(9), 2381-2391. <https://doi.org/10.1016/j.engstruct.2008.01.015>
- Vianna, J. d. C.; Costa-Neves, L.; Vellasco, P. d. S.; De Andrade, S. (2009).** Experimental assessment of Perfbond and T-Perfbond shear connectors' structural response. *Journal of Constructional Steel Research*, 65(2), 408-421. <https://doi.org/10.1016/j.jcsr.2008.02.011>

Xu, X.; Zeng, S.; He, W.; Hou, Z.; He, D.; Yang, T. (2022). Numerical Study on the Tensile Performance of Headed Stud Shear Connectors with Head-Sectional Damage. *Materials*, 15(8), 2802. <https://doi.org/10.3390/ma15082802>

Yu, Z. L.; Zhu, B.; Dou, S. T.; Liu, W. X. (2012). 3D FEM simulation analysis for PBL shear connectors. *Applied Mechanics Materials*, 170, 3449-3453. <https://doi.org/10.4028/www.scientific.net/amm.170-173.3449>

Zheng, S.; Liu, Y.; Liu, Y.; Zhao, C. (2019). Experimental and parametric study on the pull-out resistance of a notched perfbond shear connector. *Applied Sciences*, 9(4), 764. <https://doi.org/10.3390/app9040764>